Assessing coastal flooding hazard in urban areas: the case of estuarian villages in the city of Hyères-les-Palmiers

Sylvestre Le Roy[1,a], Alexis Stepanian[2], Rodrigo Pedreros[1], Thomas Bulteau[2], Alexandre Nicolae-Lerma[1], and Yann Balouin[2]

[1]*BRGM, Direction Risques et Prévention, 45060 Orléans Cedex 2, France*
[2]*BRGM, Direction des Actions Territoriales PACA (13276 Marseille), Aquitaine (33600 Pessac) and Languedoc-Roussillon (34000 Montpellier), France*

Abstract. This study, conducted on the city of Hyères-les-Palmiers (French Riviera) to guide the future land use planning, aimed to evaluate how sea level rise could modify coastal flooding hazards in urban areas located near small estuaries in a microtidal context. A joint probability approach allowed establishing typical storm parameters for specific return periods (30, 50 and 100 years), integrating offshore conditions (sea level and significant wave height) and the river level. Storm scenarios have been established from these parameters and the chronology of the most impacting recent storm. Sea level rise has been integrated (20 cm for year 2030 and 60 cm for year 2100), and the coastal flooding has been simulated with a non-hydrostatic non-linear shallow-water model (SWASH). The calculations have been realized on high resolution DEM (1 to 5 m mesh size), integrating buildings and coastal protections. The approach has been validated by reproducing a recent flooding event. Obtained results show the importance of wave overtopping in current coastal flooding hazard in this area. Nevertheless, if Hyères-les-Palmiers is currently little exposed to coastal flooding, these simulations highlight an increasing role of overflowing due to sea level rise, leading to significant flooding in 2100, even for quite frequent events.

1 Introduction

Coastal flooding simulation by wave overtopping is a rapidly developing field because of the recent progress on the numerical models (phase-resolving models), on the computer resources and the availability of high-resolution data (topographic and bathymetric LiDAR data) . These tools now allow to evolve from empirical methods (generally determined on idealized cases) to very fine simulations that can predict realistic behaviour of hydrodynamic flows and interactions with coastal defences and buildings [1, 2].

This study was conducted on behalf of the municipality of Hyères-les-Palmiers (Var), in the framework of a project concerning “trials of relocation of activities and goods (spatial reconstruction of territories threatened by coastal risks)", launched in 2012 by the French Ministry for the environment. Using these new tools, the objective was to characterize realistically coastal flooding on the territory of “Ceinturon plain” (Figure 1) and the impact of sea-level rise on the exposure of this territory to coastal flooding.

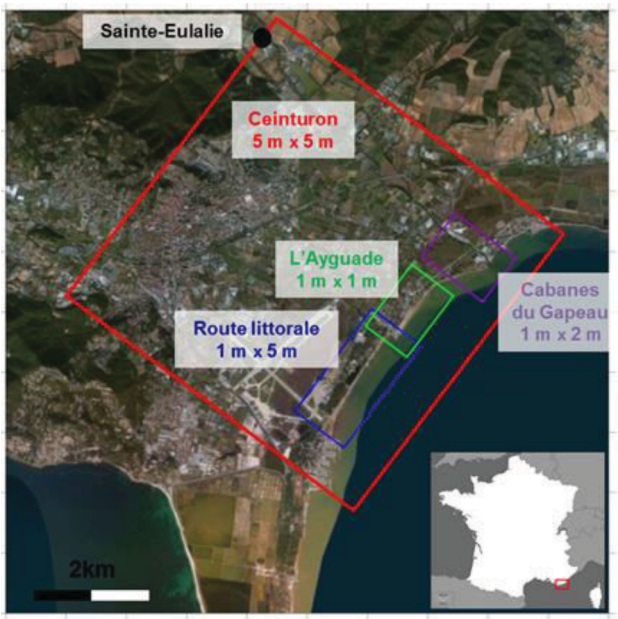

Figure 1. Studied area and extensions the different calculation grids

To this end, a numerical model was implanted, allowing the simulation of coastal flooding processes at high-resolution (taking into account buildings and walls), and allowing to represent the diversity of phenomena likely to interact during a storm event for lead to flooding of low-lying coastal zone (general overflowing, wave

[a] Corresponding author: s.leroy@brgm.fr

overtopping, simultaneity of the storm and of a flooding of the river on the site, called Gapeau).

In a first time, return periods have been determined (30, 50 and 100 years) on the basis of an analysis to joint probabilities to determine the studied scenarios. After a validation of the modeling system, the numerical simulations of these scenarios from offshore to the coastal flooding were realized to estimate the flood including the effect of rising sea level (years 2030 and 2100), and to finally analyze the future exposure of this territory to the various processes involved.

2 Scenarios definition

Seeing the objectives, an joint-probability analysis was necessary to establish return periods of studied events. Necessary parameters correspond firstly to the offshore sea conditions (sea level, significant wave heights) and also to the river level.

2.1 Available data

In the absence of tide gauge in the Hyères Bay, it was assumed that the measurements realized by the tide gauge in Toulon harbour (located about twenty kilometres) could be considered as representative of the sea levels in Hyères Bay. Sea level measurements in Toulon have been available since 1961, although there are significant gaps between late 1968 and late 2012.

The wave characterization in Hyères Bay has meanwhile been performed from a database realized elsewhere by the BRGM [3]. This database, established by spectral simulations of waves on the 1979-2009 period and validated by comparison of storm events with wave measurements, allows to characterize the waves at a hectometric resolution in Hyères area.

Finally, the river level was characterized from measurements of the water level gauge of Sainte-Eulalie, located about 5 km upstream from the estuary. Exploited measurements cover the period from late 1970 to late 2013, and are carried out continuously with an event-adaptive acquisition frequency.

2.2 Method

Preliminary analysis of the data confirmed a significant dependency between variables, justifying tri-variate joint analysis. This analysis, realized using the software Join-Sea [4], focused on the three parameters (sea level, wave HS, river level). The direction of the waves was not considered in the multivariate analysis, but preliminary statistics showed that 2 regimes were dominant (southerly waves and easterly waves), but the southerly storms proved much more rare as easterly ones is in this area.

After removing the linear long-term trend of sea level rise, the first step in the analysis is to select independent triplets, by first selecting the flood peaks (by 5-day blocks, with a minimum separation of 2.5 days between each peak to ensure their independence). For each flood peak value, the maximum sea level and waves were searched in a 2.5 days window centered on the flood peak (with minimum separation time of 1 day between the maxima of a same variable to ensure their independence). Otherwise, as each value of Hs is associated with a corresponding peak period Tp, this selection led to a number of quadruplets (HS, Tp, SWL, NR) corresponding to approximately 16.5 years of common data with 73 events / year.

After calculating the correlation coefficients between pairs of variables, the trivariate normal distribution (representative of the dependence between the 3 variables) was determined, as well as marginal distributions (specific to each variable individually) with GPD distributions. These distributions were then used to simulate with a Monte Carlo method a fictitious 100,000 years period, corresponding to 7,300,000 triplets. This fictitious series of triplets allowed to calculate the surfaces of joint-exceeding return periods (ie return periods of an event for which all the three parameters will at least exceed given data values for each parameter). For ease of reading, these surfaces were then declined in joint-exceeding iso-probability curves (Hs and sea level) for given exceeding levels of the river (Figures 2, 3 and 4).

Finally, for each necessary return period (30, 50, 100 years), a triplet was selected on the curves to provide offshore forcing conditions for studied scenarios. The choice of this triplets was guided by a number of conditions, including the fact that experience shows that the worst flooding configurations are in the bending area (high sea levels and strong waves) and that the objective of the study was to focus on coastal flooding (low river level were selected). However, the duration of the study did not allow exploring several triplets for a given return period. The synthesis of selected parameters is shown in Table 1.

Parameter	Tr=30 yr Year 2030	Tr=30 yr Year 2100	Tr=50 yr Year 2100	Tr=100 yr Year 2100
Current sea level SWL (m above the lowest tides)	*0.95*	*0.95*	*0.95*	*0.95*
Wave significant height Hs (m)	*4.50*	*4.50*	*4.71*	*4.99*
River level in Sainte-Eulalie NR (m)	*0.50*	*0.50*	*0.50*	*0.50*
Sea-level rise (m)	*+0.20*	*+0.60*	*+0.60*	*+0.60*
Resulting sea level (m, French General leveling)	*0.90*	*1.30*	*1.30*	*1.30*

Table 1. Selected parameters for studying scenarios of given return-periods at a given deadline.

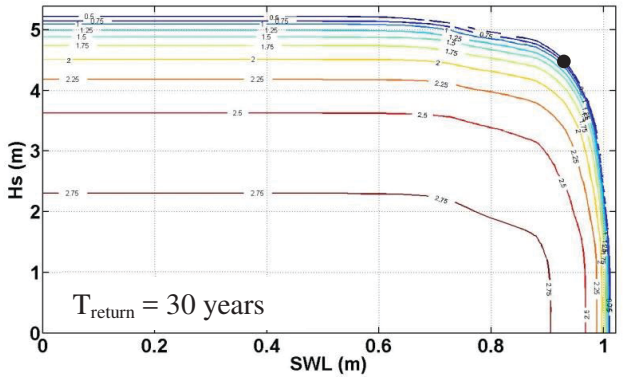

Figure 2. 30-years return period contours of joint exceeding parameters for SWL (sea level), Hs (wave significant height) and NR (river level, indicated on each curve); the black dot represents the selected triplet for a 30-years return period.

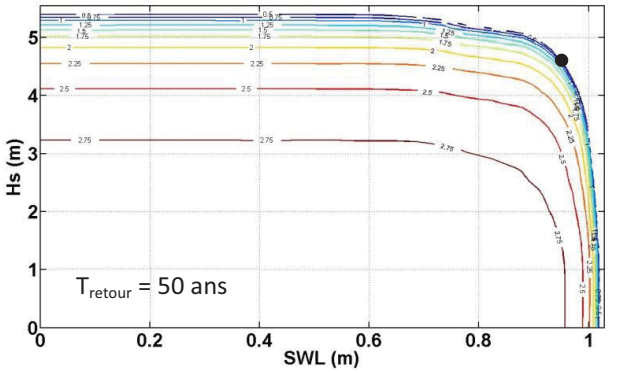

Figure 3. 50-years return period contours of joint exceeding parameters for SWL (sea level), Hs (wave significant height) and NR (river level, indicated on each curve); the black dot represents the selected triplet for a 50-years return period.

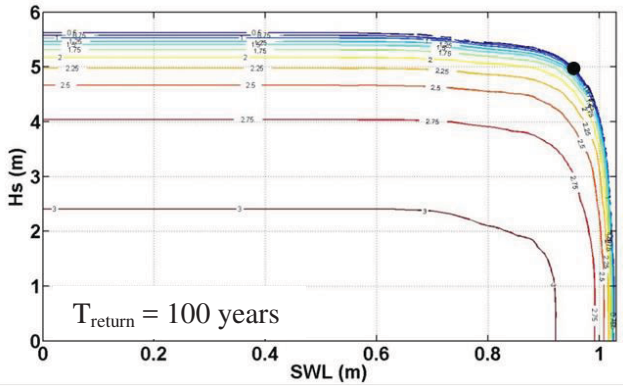

Figure 4. 100-years return period contours of joint exceeding parameters for SWL (sea level), Hs (wave significant height) and NR (river level, indicated on each curve); the black dot represents the selected triplet for a100-years return period.

2.3 Chronology

The analysis of the chronologies of some recent storms (October 1999, December 2008, December 2009) showed that the phase shifts between the different phenomena (river flows, sea levels, waves) could be very variable: if the peak of the waves occurs almost synchronous with the maximum sea levels (within a few hours under the influence of the tide), the river peak may be shifted significantly later (from several hours to over 12 hours). Consequently, it was therefore chosen to simply use the chronology of the only known recent storm that caused significant flooding (December 2008), slightly modified to make waves and sea level peaks perfectly concomitant.

Parameters chronologies during this storm have been standardized over a period of 2.5 days. This standard chronology has then been applied to each scenario, taking into account their specific parameters and setting "normal" values (that is to say off-storm).

Sea level rise as a result of climate change was then superimposed on sea level chronology, resulting in sea levels before and after the storm that includes this elevation.

The wave period was also estimated directly from the dependency relationship with HS established in the statistical analysis.

2.4 Results

This approach ultimately allowed to define forcing conditions for the modeling chain, in the form of time series of sea level, offshore wave heights and upstream river levels (which finally remains constant) . Examples of the forcing conditions imposed for the 30 years return period at 2030 deadline scenario and for the 100 years return period at 2100 deadline scenario are illustrated in Figures 5 and 6. The wave peak period was directly deducted from their significant heights from the centerline curve of peak periods according to significant heights (generated from the simulation 100 000 years of fictitious data).

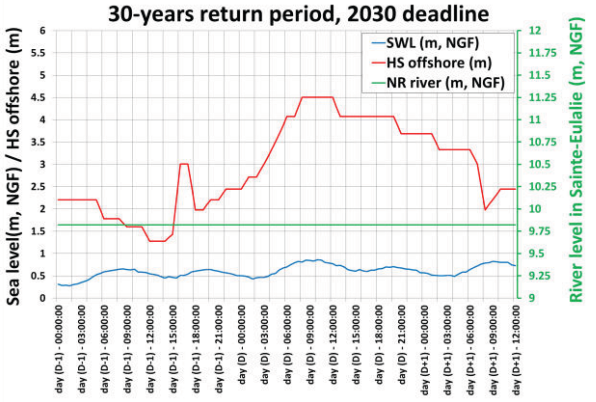

Figure 5. Forcing conditions for the 30 years return period at 2030 deadline scenario.

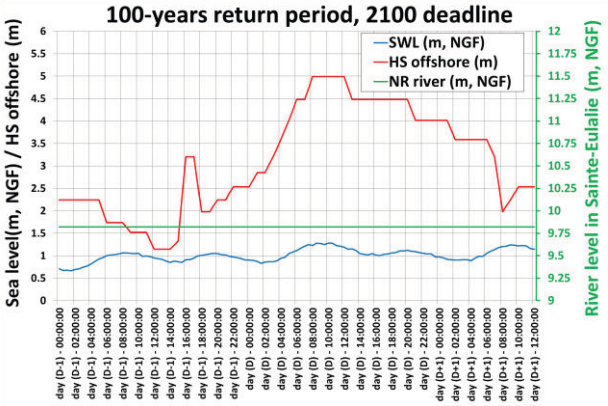

Figure 6. Forcing conditions for the 100 years return period at 2100 deadline scenario.

3 Coastal flooding simulations

Modeling strategy is based on a downscaling and on the choice of the parameters to be considered according to the area and to the configuration. This strategy has been applied to the storm of December 2008 for validation, and then to the selected scenarios for the study.

3.1 Wave propagation until the coast

Due to wave transformation while approaching the coast, wave characteristics (determined offshore in the joint probabilities analysis) must be propagated to the coast using a spectral model, with sufficient resolution to capture the changes they undergo when the depth is reduced.

The spectral model SWAN, based on the spectral equation of conservation of wave action that is resolved following an implicit finite difference scheme [5], has been implanted to cover the western part of the Hyères Bay with a resolution of 20 m, the eastern limit corresponding to the point where the waves were characterized in the joint probabilities analysis (Figure 7).

The previously determined scenarios were then simulated, with the following assumptions:
- The source of waves is eastern sector;
- The waves were assumed to be homogeneous along the eastern limit;
- The wave period was directly deducted from their significant height by the dependent relationship established during the statistical analysis;
- Simulations for each scenario were performed in unsteady conditions (water levels and waves) over a period of 2.5 days, and include sea level rise associated with each scenario.

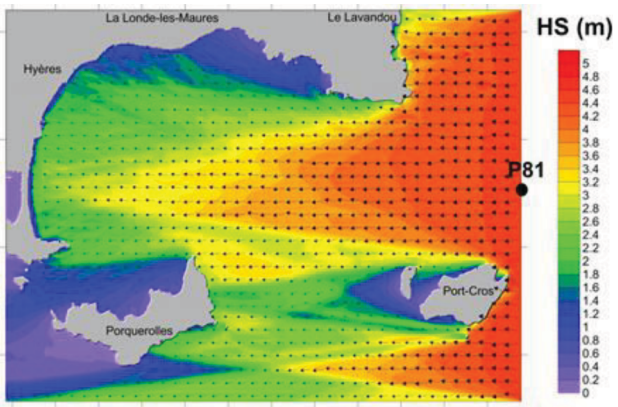

Figure 7. Calculation area for wave spectral simulations: Example of the wave significant heights at the peak of the storm for the scenario of return period 30 years at the 2030 deadline.

3.2 Model

SWASH is a free access phase resolving model (otherwise called "wave to wave") developed by the Delft University of Technology [6]. It resolves the nonlinear shallow-water equations (NLSW) including non-hydrostatic pressure terms. This code simulates the propagation of waves in coastal area and the onshore coastal flooding as it takes into account the phenomena of refraction, diffraction, bottom friction, swelling, flood, reflection, interaction (wave-wave, wave-current), generation of currents induced by the waves, treatment of wet-dry interface in the swash zone and flows propagation in the presence of structures and buildings. A preview of the wave propagation simulation and associated flooding with SWASH on the study area is presented in Figure 8.

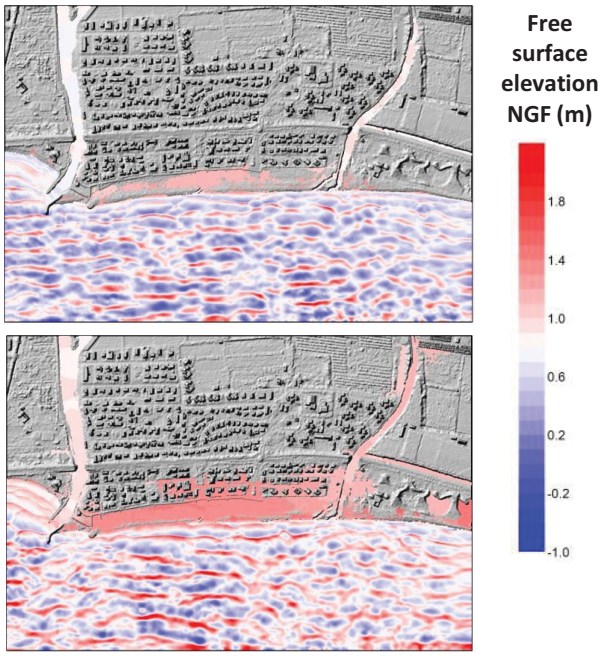

Figure 8. Snapshots of a SWASH simulation on the hamlet of L'Ayguade.

3.3 Input data

To simulate as fine as possible the complex phenomena on the study area, several computational grids were used, covering variable areas with variable resolutions following the considered area and the implied phenomena (Figure 1):
- The largest grid covers the entire Ceinturon plain, and extends to Sainte-Eulalie to allow the simulation of the flow of the Gapeau river. This grid only simulates overflow phenomena (marine and/or river) at a 5 m-resolution (the dynamic component of the waves is not simulated). The grid is defined through a digital terrain model (DTM, with no explicit buildings in the topography), mainly realized from LiDAR data and available topographic and bathymetric (sea and river) data.
- On the whole coastline of the Ceinturon plain, high resolution simulations were realized, including this time the dynamic component of the waves. This required the use of 3 computation grids with reduced footprints, covering respectively, from south to north, the coastal road, the hamlet of L'Ayguade and the hamlet of "Cabanes du Gapeau". These grids correspond this time to digital elevation models (DEM, including buildings and some walls in the topography). They were realized

from LiDAR data (treated with LASTools software, [7]) completed with additional available data (topographic and bathymetric acquisitions, field survey, buildings footprints from the french database BDTopo © IGN...). An example of the DEM realized on the hamlet of L'Ayguade, cleaned of the unsustainable elements of land use and of the elements that are unable to interact significantly with the water flows, is shown in Figure 9.

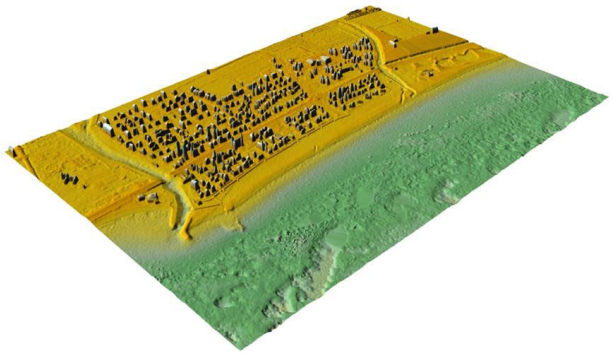

Figure 9. Digital elevation model on the hamlet of l'Ayguade, including buildings and walls.

In addition to these DTM and DEM, a map of land use covering the territory has been converted in terms of friction grids through Manning coefficients representing the ground roughness according to its use: the complex initial land-use typology has been declined in a simplified typology (according to soil roughness), for which each category has received a given Manning coefficient inspired from scientific bibliography (especially [8, 9, 10], Table 2). Urban areas received a special treatment as they received high Manning coefficients (0.1 to 0.4 $s/m^{1/3}$) on the large grid (DTM) to represent the strong roughness induced by buildings (Figure 10), whereas low Manning coefficient values were used (0.016 $s/m^{1/3}$) for the more resolved grids (DEM), rather representative of the concrete, since the buildings were incorporated directly into DEM.

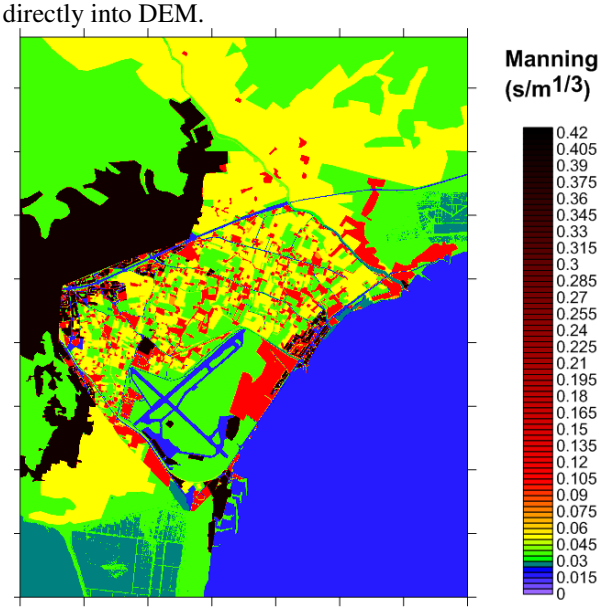

Figure 10. Map of the Manning coefficients attributed to the large calculation grid (5m-resolution) according to the soil-use

3.4 Model forcing

Forcing conditions for each computation grid are deducted directly from scenarios identified in the probabilistic analysis (§ 2.4) and from the simulation of wave propagation through the Hyères Bay (§ 3.1).

Simplified typology	Manning coefficient ($s/m^{1/3}$)
Concrete, asphalt	0.016
Meadows	0.04
Crop fields	0.05
Dense urban area	0.4
Sparse urban area	0.1
Dense forest	0.1
Sparse forest	0.04
Water surface	0.03
Strongly rough soil (forest cutting, dumping ground, precarious buildings…)	0.07
Moderately rough soil (construction sites, tracks…)	0.045
Weakly rough soil (beaches, dunes, stone…)	0.03

Table 2. Attribution of Manning coefficients according to land-use and soil nature

Thus, the 5 meter-resolution simulation (Ceinturon Plain) is forced on the one hand by the evolutions of the river level (in the north) and on the other hand by the evolutions of the sea level (including wave-setup caused by wave breaking near the coast, and calculated in the spectral simulations) on the marine side (south), as illustrated in Figure 11.

The finer calculations ranks are forced by the evolutions of the sea level and of the wave characteristics near the coast. In addition, for the grid covering the hamlet of "Cabanes du Gapeau" (corresponding to the estuary of the river), the river level is forced by the river level derived from the 5 m-resolution simulation (Figure 12).

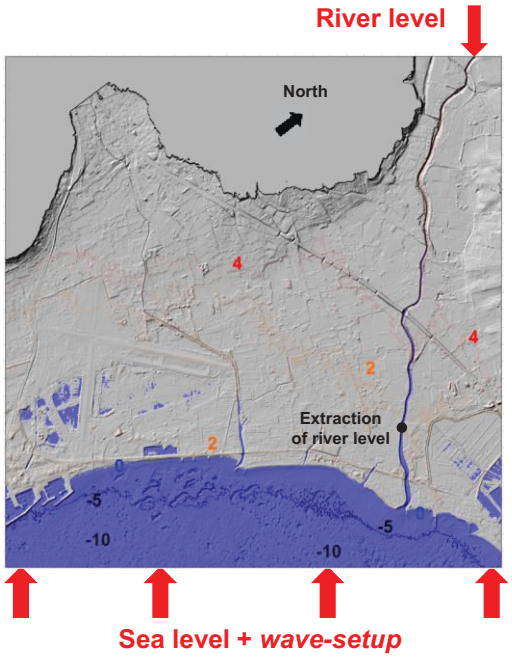

Figure 11. Forcing imposed to the larger grid (5m-resolution) and position of the extraction point for imposing the river level in the finer grid on Cabanes du Gapeau

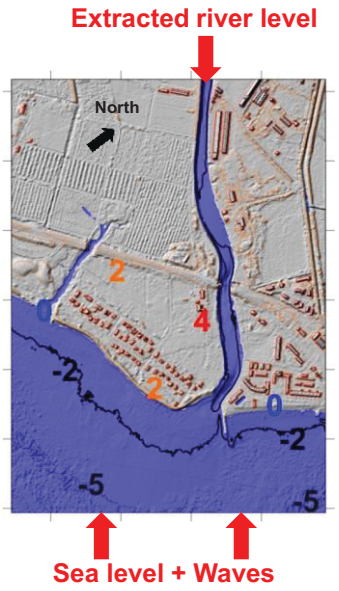

Figure 12. Forcing imposed to the finer grid on the hamlet of Cabanes du Gapeau.

3.5 Validation

The modeling strategy was validated through an application on a real event. As observed coastal flooding on this area remain very scarce, the storm that occurred on December 14th, 2008 was chosen because of wave overtopping observed in L'Ayguade. This is the only recent storm that caused a significant coastal flooding (but very limited, with flood heights from a few centimeters to a few decimeters). It should be noted that unlike classical storms in the studied area (which are eastern sector), the December 2008 storm is a southern storm. Wave propagation characteristics was realistically simulated with SWAN, by simply adding an extra calculation rank of 20 m resolution (§ 3.1) to the simulations conducted by [3].

The flooding simulations on the large rank (5 m-resolution) proves consistent with the observations (no significant overflow, either from the river or from the sea side, even if sea level in the estuary reveals to be very close to the top of the docks).

The flood simulation very high resolution in the hamlet of L'Ayguade also appears consistent with the available evidences, although the flood seems to be slightly underestimated: the flood is caused by wave overtopping, limited to the holes in the wall on the top of the beach (pedestrian passages), leading to flooding of several centimeters to several tens of centimeters in the seaside streets (Figure 13). Underestimation in the simulation could be explained by the very small intensity of the studied event, with inland water heights of the same order as the estimated accuracy of LiDAR data (about 10 to 20 centimeters).

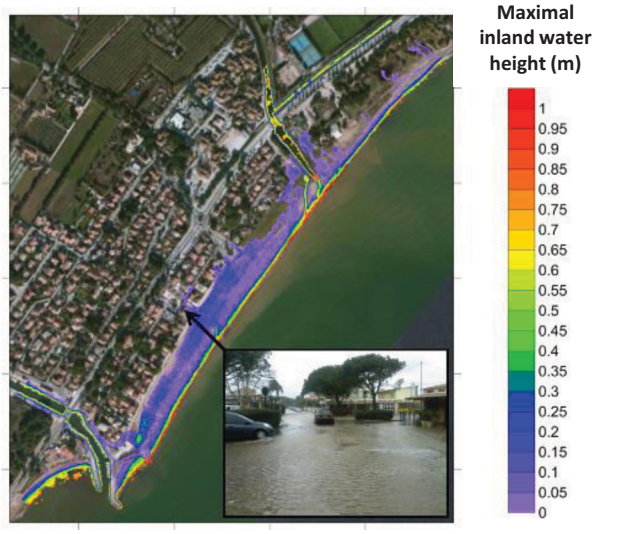

Figure 13. Maximal simulated water heights inland in the hamlet of L'Ayguade during December 2008 storm and comparison with a photography during the event (Photography from the Hyères municipality).

4 Results

The simulations have been carried out on each calculation grid for each considered scenario. The centennial scenario for 2100 deadline was simulated by considering widespread destruction of protective structures (here the wall on the top of the beach in L'Ayguade and a riprap in Cabanes du Gapeau).

The large simulations on the Ceinturon Plain show that the river contributes in a limited way to overflow in the estuary (the river outflow remains limited in the scenarios). The very high resolution simulations allow highlighting a number of conclusions on the study site:

- The site, although currently little affected by coastal flooding, could be significantly impacted in the future as a result of climate change (especially the hamlets of L'Ayguade and Cabanes Gapeau);
- The relative roles of the various processes show that if wave overtopping may be significant in short term (even for relatively frequent events, Figure 14), overflowing

becomes the dominant process in long term under the effect of sea level rise (Figure 15), the waves revealing then less important;
- Local structures can have a significant impact on coastal flooding, whether in terms of protection (protection structures, in the assumption that they resist) or in terms of weakness (failure of protection structures, presence of estuaries and valleys, locally named "lônes", which allow an overflow in low areas behind urban areas leading to a larger propagation of the flooding in these areas, for example, see Figures 16 and 17, in the hamlet of Cabanes du Gapeau).

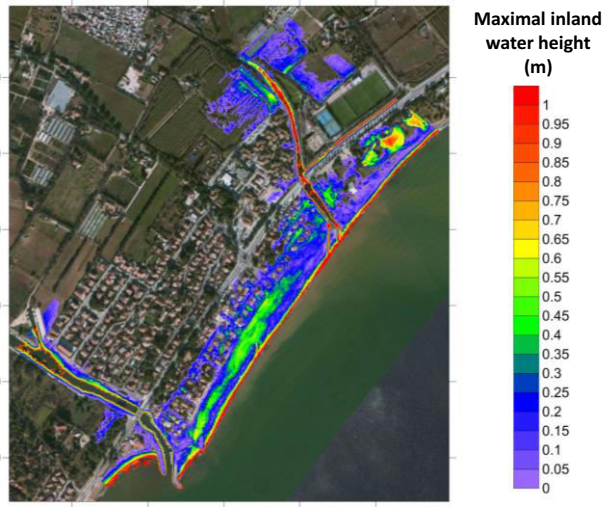

Figure 14. Maximal simulated water heights inland in the hamlet of L'Ayguade for a return period of 30 years at 2030 deadline.

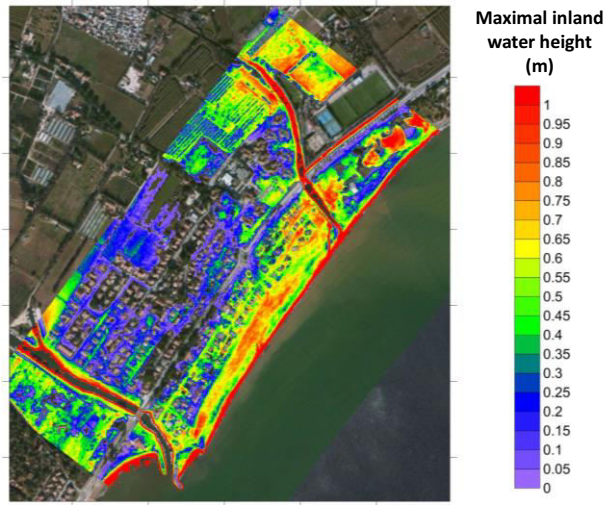

Figure 15. Maximal simulated water heights inland in the hamlet of L'Ayguade for a return period of 100 years at 2100 deadline.

5 Conclusions

These results, more than the specific conclusions for the studied site, show that new digital tools in addition to the availability of very high resolution data make now possible to realistically simulate the complexity of the phenomena involved in coastal flooding, including in the context of small estuaries in micro-tidal context. The quantification of climate change impacts becomes conceivable (however with some assumptions, here for example the fact that the statistics produced on the current remain valid in the future), and can show that some sectors currently relatively spared by this hazard could in the future become significantly exposed.

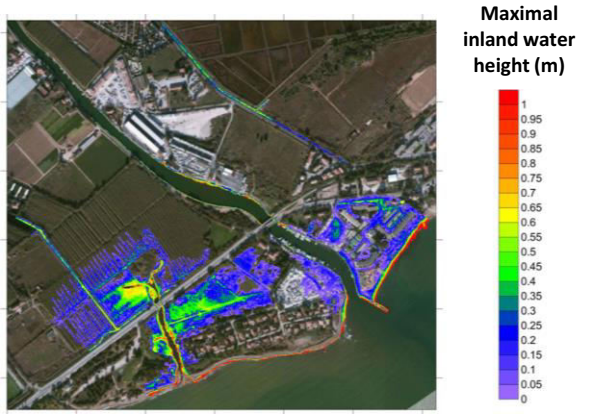

Figure 16. Maximal simulated water heights inland in the hamlet of Cabanes du Gapeau for a return period of 30 years at 2030 deadline.

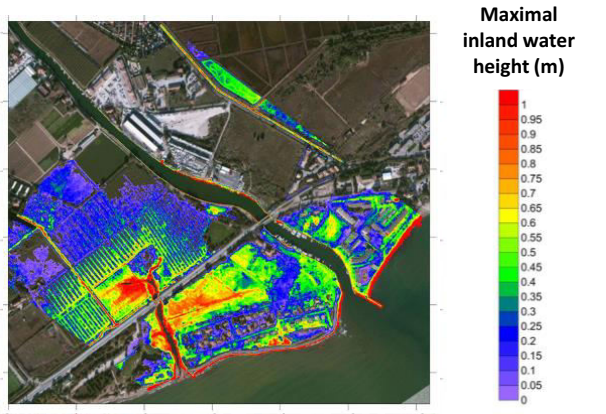

Figure 17. Maximal simulated water heights inland in the hamlet of Cabanes du Gapeau for a return period of 30 years at 2030 deadline (top) and for a return period of 100 years at 2100 deadline (down).

6 References

1. Le Roy S., Pedreros R., André C., Paris F., Lecacheux S., Marche F. and Vinchon C. (2015). Coastal flooding of urban areas by overtopping : dynamic modelling application to the Johanna storm (2008) in Gâvres (France). *Natural Hazards and Earth System Sciences*, **Vol. 15**, pp. 2497-2510.
2. Pedreros R., Vinchon C., Lecacheux S., Delvallée E., Balouin Y., Garcin M., Krien Y., Le Cozannet G., Poisson B., Thiebot J., Bonneton P. and Marche F. (2011). Multi models approach to assess coastal exposure to marine inundation within a global change context. *EGU (European Geosciences Union) General Assembly, Wien, 3–8 April 2011*, Poster.
3. Stepanian A., Lecacheux S., Nicolae-Lerma A. and Pedreros R. (2014). Evaluation des Risques Naturels Littoraux sur le territoire du SCoT Provence-Méditerranée – Caractérisation de l'aléa submersion marine. *Rapport BRGM/RP-63949-FR*, 119 p. (in french).

4. HR WALLINGFORD and Lancaster University (2000). The Joint Probability of Waves and Water Levels: JOIN-SEA - A rigorous but practical new approach. *Report SR537*.
5. Booij N., Haagsma IJ.G., Holthuijsen L.H., Kieftenburg AT.M.M, Ris R.C., Van Der Westhuysen A.J. and Zijlema M. (2004). Swan Cycle III version 40.41. *User's Manual*, 115 p.
6. Zijlema M., Stelling G. and Smit P. (2011). SWASH: An operational public domain code for simulating wave fields and rapidly varied flows in coastal waters. *Coastal Engineering*, **Vol. 58**, pp 992–1012.
7. Hug C., Krzystek P. and Fuchsc W. (2004). Advanced LiDAR data processing with LasTools. *XXth ISPRS Congress, 12-23. July 2004, Istanbul, Turkey.*
8. Chow V.T. (1959). Open-channel hydraulics. *New York, McGraw-Hill*, 680 p.
9. Engineers Australia – Water engineering (2012). « Australian Rainfall & Runoff » - Project 15: Two dimensional modeling in urban and rural floodplains. *Stage 1&2 report P15/S1/009*, November 2012.
10. Bunya S., Dietrich J.C., Westerink J.J., Ebersole B.A., Smith J.M., Atkinson J.H., Jensen R., Resio D.T., Luettich R.A., Dawson C., Cardone V.J., Cox A.T., Powell M.D., Westerink H.J., Roberts H.J. (2010). A High-Resolution Coupled Riverine Flow, Tide, Wind, Wind Wave and Storm Surge Model for Southern Louisiana and Mississippi: Part I – Model Development and Validation. *Monthly Weather Review*, **Vol. 138**, 345-377.